Journal of Medicinal Chemistry
Brief Article

J. Med. Chem. **2010,** *53,* 509–513 **509**
DOI: 10.1021/jm9011092

Novel Organic Proteasome Inhibitors Identified by Virtual and in Vitro Screening

Nicolas Basse,[†,∥] Matthieu Montes,[‡,∥] Xavier Maréchal,[†] Lixian Qin,[†] Michelle Bouvier-Durand,[†] Emilie Genin,[§] Joëlle Vidal,[§] Bruno O. Villoutreix,*[,‡] and Michèle Reboud-Ravaux*[,†]

[†]*Enzymologie Moléculaire et Fonctionnelle, UR4, UPMC-Université de Paris 6, Case 256, 7 Quai Saint Bernard, F 75252 Paris Cedex 05, France,* [‡]*Inserm UMR-S 973, Molécules Thérapeutiques in Silico, Université Paris Diderot, 35 rue Hélène Brion, 75013 Paris, France, and* [§]*Chimie et Photonique Moléculaires, CNRS-UMR 6510, Université de Rennes 1, Campus Beaulieu, Bât. 10A, case 1012, CS 74205, 35042 Rennes Cedex, France.* [∥]*Present addresses. For N.B.: MRC Laboratory of Molecular Biology, Hills Road, Cambridge CB2 0QH, U.K. For M.M.: Conservatoire National des Arts et Métiers, 292 Rue Saint Martin, 75003 Paris, France.*

Received July 2, 2009

Proteasome inhibition is a promising strategy for treating cancers. Herein, we report the discovery of novel drug-like inhibitors of mammalian proteasome 20S using a multistep structure-based virtual ligand screening strategy. Sulfone- or piperazine-containing hits essentially belong to the under-represented class of noncovalent and nonpeptidic proteasome inhibitors. Several of our compounds act in the micromolar range and are cytotoxic on human tumoral cell lines. Optimization of these molecules could lead to better anticancer therapy.

Introduction

The 20S proteasome is a multicatalytic protease playing a crucial role in cellular protein turnover in eukaryotes. It is involved in the maintenance of the biological homeostasis and degradation of key components of the cell machinery. Critical cellular functions such as transcription, cell-cycle progression, cell differenciation, antigen processing, and tumor suppression rely on this molecular system.[1,2] Regulation of the proteasome activity by specific molecules is of therapeutic interest, particularly in cancer.[3,4] The peptide boronate bortezomib is a prescription drug against multiple myeloma and mantle lymphoma diseases that are generally fatal within a year if not treated.[5] However, resistance and adverse effects of the chemotherapy making use of bortezomib are of continual concern.[6] As bortezomib (Figure 1 top left), most available inhibitors of the proteasome form a covalent bond with the active site Thr1O$^{\gamma}$ of the β-subunits.[7] Noncovalent inhibitors of the proteasome have been less extensively investigated. They include ritonavir,[8] aminobenzylstatine,[9] and 3,4,5-trimethoxy-L-phenylalanine derivatives,[10] lipopeptides,[11] macrocyclic[12] (Figure 1 bottom left) and linear[13] **1** (TMC-95A)[14] derivatives, and fluorinated pseudopeptides.[15] These molecules have the advantage to be devoid of a functional group usually prone to nucleophilic attack because reactive warhead groups are often associated to drawbacks such as lack of specificity, excessive reactivity, and instability. Yet, all these previously reported inhibitors are peptide derivatives and it would be very valuable to also develop more "drug-like" molecules against this enzyme. We present here the identification and biological evaluation of organic inhibitors of mammalian 20S proteasome using a virtual ligand screening approach. The molecules belong to new chemical classes of inhibitors acting preferentially with the proteasome through noncovalent interactions.

Results and Discussion

Designing drug-like inhibitors for the proteasome target is very challenging[12] because the different active sites can accommodate a large variety of peptide substrates and inhibitors (Figure 1). In the present study, we first screened the CT-L active site using different computational tools. The CT-L binding pocket is relatively polar with a polarity ratio of 0.30 (e.g., an hydrophobic pocket would have a polarity ratio of around 0.15) and has an overall volume of about 1500 Å^3 (while the investigated drug-like molecules have a volume of about 400 Å^3). We decided to run several test cases to ensure that the docking-scoring engines used in this study could reproduce known experimental structures of the proteasome cocrystallized with covalent compounds. For instance, we docked bortezomib with Surflex,[16] assuming that prior to forming a covalent bond with Thr1, the molecule has to bind to the CT-L site like a noncovalent inhibitor. The best Surflex pose (best energy among 30 generated binding modes) positioned the compound in a manner highly similar to the one observed in crystallographic studies but for the boronic acid moiety that should form a covalent bond with Thr1 (see Figure 1 in Supporting Information). Yet, this chemical group is only slightly shifted as compared to the X-ray structures.[17] The Surflex scores were between 8 and 9, which is also interesting as for many compounds that do not bind to the CT-L site, the scores were around 3. Clearly, none of the presently developed scoring functions are fully reliable nor do they fully correlate with experimental affinity, however, these initial results were encouraging. We ultimately decided to carry out a multistep protocol chaining several docking-scoring engines (FRED, LigandFit, Surflex) and we used a compound collection (Chembridge) that contained about 300000 molecules after in silico ADME/Tox filtering. We selected, after docking/scoring and visual inspection,

*To whom correspondence should be addressed. For B.V.: phone, +33 157278386; fax, +33 157 27 83 72; E-mail, Bruno.Villoutreix@inserm.fr. For M.R.R.: phone, +33 1 44 27 50 78; fax, +33 1 44 27 50 22; E-mail, michele.reboud@upmc.fr.

Published on Web 11/17/2009

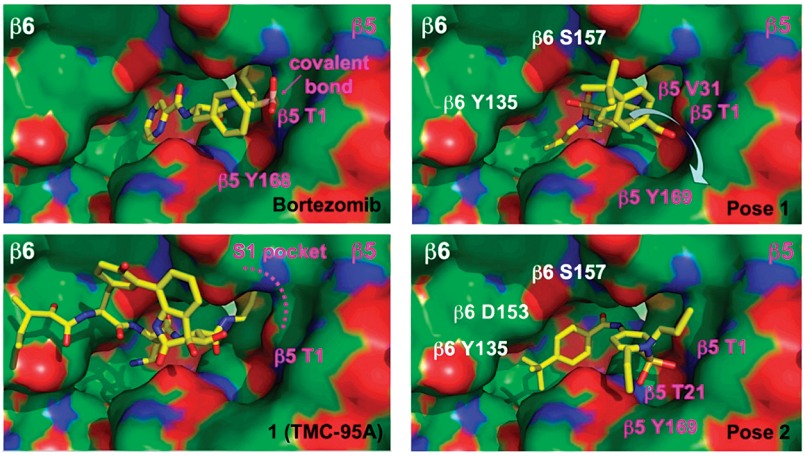

Figure 1. Structure of bortezomib (top left) and **1** (bottom left) were positioned into the CT-L pocket by superimposing the appropriate yeast proteasome X-ray structures onto the bovine proteasome experimental structure. The binding pocket is shown as solid surface with carbon atoms colored green, N, blue, and O, red. The small molecule color-code is as follow, C, yellow, N, blue, O, red, and B, pink. Bortezomib makes a covalent bond with Thr1. Pictures to the right represent two likely binding modes for molecule **2b**. In pose 1, hydrogen bonds are formed with Ser157, Arg19, Thr1. A slight structural change would lead to favorable aromatic and hydrophobic interactions between molecule **2b** and Tyr169. Weak hydrophobic interactions are also noticed with Tyr135. In the case of pose 2, hydrogen bonds were found between the compound and Thr21 and Thr1. Some other residues are labeled for orientation.

Chart 1. Structure of Compounds **2**−**8**

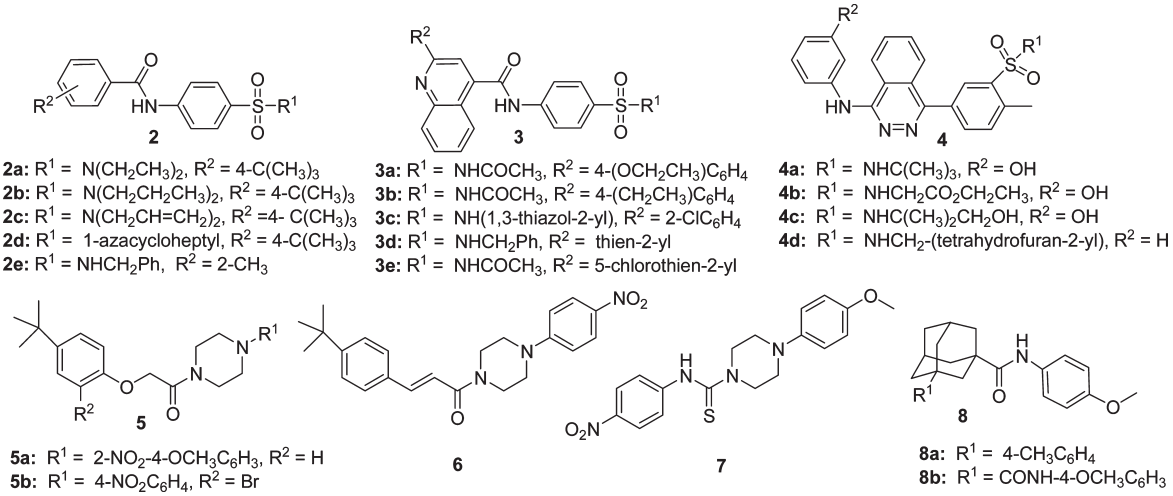

200 molecules for experimental testing against the CT-L activity of the rabbit 20S proteasome. PA and T-L activities were also investigated using the appropriate fluorogenic substrates. The aldehyde proteasome inhibitor MG132[18] (Z-LLL-H) was used as standard.[13] Structures and inhibition efficacies of the most active compounds are summarized in Chart 1 and Table 1. Thirteen of the 200 tested compounds were inhibiting the CT-L activity, yielding a reasonable hit rate of 6.5% [(13/200) × 100]. Finally, a total of 20 compounds inhibited at least one proteasomal activity (i.e., frequently, proteasome inhibitors acting against one type of catalytic site cross react with another type). Some compounds inhibited three activities (**2c**, **3c**, **4a**−**c**), two activities (**2a**−**b**, **2d**−**e**, **3a**−**b**, **7**, **8a**−**b**), or only one (**4d**, **5a**−**b**). Five compounds exhibited IC_{50} values below 20 μM. Examination of active compounds revealed a diversity of chemical structures (Table 1). The structural feature that is common to 14 compounds (**2**−**4**) is a sulfonamide group. Compounds **2**−**3** are sulfanilic acid derivatives, *N*-acylated by a 4-substituted benzoyl group (**2**) or a quinoline-4-carbonyl group (**3**). The sulfonyl R^1 substituent is a monosubstituted (**2e**, **3a**−**e**) or a disubstituted (**2a**−**d**) amino radical. Three other chemical classes are constituted by 4-arylsulfonylphthalazines (**4**), monoacylated or monothioacylated piperazines (**5**−**7**) and adamantanecarboxamide derivatives (**8**). In the sulfonamide series **2**−**3**, compounds **2b** (Figure 1, Supporting Information Figure 2) and **2c** with the branched aliphatic chains R^1 $N(CH_2CH_2CH_3)_2$ and $N(CH_2CH{=}CH_2)_2$, respectively, gave better inhibition of CT-L and PA activities than did shorter aliphatic chains (R^1 = $N(CH_2CH_3)_2$, **2a**; $NHCOCH_3$, **3a**−**b**) and saturated (cycloheptane, **2d**) or aromatic (**2e**, **3d**) cycles. The thiazole group (R^1 = NH-thiazole, **3c**; IC_{50} of 23.3 μM on PA activity) favored the inhibition of PA activity rather than that of CT-L activity. The nature of the R^1 substituent of the sulfonyl group was also important in the arylsulfonylphthalazine series **4** because the tetrahydrofurane substituent (**4d**) was less favorable than aliphatic chains (**4a**−**c**). In the piperazine series, the thioureido compound (**7**) was the best inhibitor (IC_{50} of 10.8 ± 0.9 and 9.0 ± 1.2 μM for CT-L and PA activities, respectively) (see Figure 3 in Supporting Information). The adamantanecarboxamide derivative **8b** was more efficient on CT-L and PA activities

Table 1. Inhibition of Rabbit 20S Proteasome at pH 8 and 37 °C[a]

	IC_{50} (μM) or % inhibition ([I] = 50 μM)		
compd	CT-L	PA	T-L
2a	87%[c]	> 25	nd[b]
2b	18.9 ± 2.9	8.0 ± 1.4	nd[b]
2c	1.9 ± 1.2	10.0 ± 4.4	4.5 ± 0.3
2d	> 50	63%[c]	nd[b]
2e	ni[b]	54%	13%[c]
3a	ni[b]	42%[c]	45%
3b	ni[b]	45%[c]	25.6 ± 1.1
3c	23%	23.3 ± 6.8	50%[c]
3d	70.1%	ni[b]	nd[b]
4a	28.3 ± 1.5	29%	44%
4b	35%	39.0 ± 13.7	63%[c]
4c	35.4 ± 2.0	14.8 ± 1.3	67.8 ± 1.4
4d	ni[b]	52%	nd[b]
5a	40%	ni	nd[b]
5b	ni[b]	49%	ni[b]
6	ni[b]	52%	ni[b]
7	10.8 ± 0.9	9.0 ± 1.2	nd[b]
8a	26.2 ± 2.8	≈50	nd[b]
8b	11.7 ± 1.4	12.4 ± 0.6	nd[b]

[a] The inhibition was evaluated after 15 min incubation of the enzyme with the inhibitor before adding the appropriate fluorogenic substrate to evaluate the remaining CT-L, PA or T-L activity. [b] ni: no inhibition; nd: not determined. [c] [I] = 100 μM.

than derivative **8a**. The reversible character of the inhibition was demonstrated for compounds **3** and **4**. The inhibited enzyme (> 80% at time 15 min) reactivated instantaneously and completely upon dilution with buffer of the reaction mixture containing the enzyme plus the inhibitor after 15 min incubation (dilution factor of 10). For these compounds, a time-independent inhibition was observed when the remaining activity was determined at intervals of time (20 s to 45 min) after the enzyme−inhibitor incubation. Conversely, a slow time-dependent inhibition was observed for compounds 2 (for example, $k_{obs}/[I] \approx 30\ M^{-1} \cdot s^{-1}$ for compound **2b**; k_{obs} is the pseudo-first-order inhibition constant characterizing the inhibition process). No subsequent reactivation was observed during 200 min after dilution of the reaction medium, suggesting an irreversible process for the corresponding compounds. Moreover, the selectivity of action on the proteasome enzyme was analyzed by checking the inhibitory potency against the competing cytosolic calpain I. This enzyme was not inhibited by compounds **2b** and **2c** (50 and 100 μM).

We investigated the binding mode of a promising inhibitor, compound **2b** (Figure 1), in an attempt to gain preliminary structure−function insights. The molecule was fully redocked with the new version of Surflex[16] and energy minimized in the binding pocket with MolDock.[19] Energetic and structural analyses suggested two possible binding modes, one with the *tert*-butylbenzene located next to Thr1 (Figure 1, pose 1, and Supporting Information Figure 2, pose 1, MolDock interaction energy = −101, arbitrary unit), the other (pose 2) with this very same group in contact with the β-6 subunit (Figure 1, MolDock interaction energy = −115). In the case of pose 1, three favorable hydrogen bonds are predicted (H-bond energy = −12.1 kcal/mol). The ligand internal energy strain is around 8.5 kcal/mol, value ranges that we observed on numerous X-ray structures with MolDock (unpublished data). For pose 2, four hydrogen bonds are expected and the hydrogen bond interaction energy between the molecule and the binding pocket was computed to be −10.3 kcal/mol while the ligand internal energy strain was around 10.5. In an attempt to investigate further the most likely binding mode of compound **2b**, we docked this molecule into the PA site. There, two main orientations were observed, approximately similar to the ones reported for the chymotrypsin-like pocket with similar Surflex scores (data not shown). Although the activity of compound **2b** was not assessed on the trypsin-like site, we also docked it at this site and the Surflex scores were similar to the ones computed for the other catalytic sites, but in this case, the ligand was somewhat locked away from the catalytic threonine (data not shown). Thus, either this molecule is not a good binder for this site or receptor flexibility would be required to fully fit into the binding pocket. Overall, in spite of such structural analysis, two main binding poses are expected for compound **2b**, and we cannot discriminate at this stage among the two. Yet, this computer simulation is in agreement with the experimental work with regard to inhibition of the PA site. X-ray crystallography experiments are undergoing to clarify this point.

The cytotoxic effects on HeLa and HEK-293 tumor cell lines were also demonstrated. Survival curves yielded for the sulfonamide compounds: compound **2b**, EC_{50} = 9.0 ± 0.5 μM (HeLa cells) and < 5 μM (HEK-293 cells), and compound **2c**, EC_{50} = 12.3 ± 0.4 μM (HeLa cells) and 9.7 ± 0.2 μM (HEK-293 cells); for the arylsulfonylphthalazine series: compound **4a**, EC_{50} = 10.4 ± 0.7 μM (HEK-293 cells); **3e**, $EC_{50} \approx 100$ μM (HeLa cells); $EC_{50} \approx 75$ μM (HEK-293 cells); **4b**, EC_{50} = 13.9 ± 1.0 μM (HEK-293 cells); for the piperazine compound **7** $EC_{50} \approx 50$ μM (HEK-293 cells).

Conclusion

We have identified several drug-like inhibitors of the proteasome using a multistep in silico screening protocol and in vitro experiments. By acting on one, two or three active site(s), these inhibitors may differentially reduce protein degradation and help to control normal cell cytotoxicity.[20] These molecules can now be optimized in order to improve their potency as potential novel anticancer drugs.

Experimental Section

In Silico Screening. The crystal structure of bovine proteasome was retrieved from the Protein Data Bank[21] (PDB[a] code 1IRU)[22] (the human protein is identical to the bovine one in the area of the binding pocket). As the CT-L active site involves two subunits (β5 and β6), we selected the chains L and M from this structure for the structural analysis and the docking experiments. All heteroatoms were removed from the file, and hydrogen atoms were added using the program InsightII (Accelrys Inc., San Diego, CA) assuming standard protonation state at physiological pH for the titratable residues (i.e., D, E, K, R). The search space for the docking study was initially defined around the catalytic threonine 1 of the CT-L active site and further refined after transposition of **1** (noncovalent inhibitor) and of the bortezomib molecule (covalent bond to Thr 1) from the yeast proteasome structure (reviewed by Borissenko and Groll)[7]. The rmsd between the yeast and bovine structures for the Cα trace for these two subunits is around 0.6 Å, thus making the process straightforward. The VLS experiments employed a multistep hierarchical protocol developed in our group[23,24] and involved the combination of three in silico screening packages:

[a] Abbreviations: AMC, 7-amino-4-methylcoumarin; DMEM, Dulbecco's Modified Eagle Medium; β-NA, β-naphthylamide; PDB, Protein Data Bank; PMS, phenazine methosulfate; XTT, 2,3-bis-(2-methoxy-4-nitro-5-sulfophenyl)-2*H*-tetrazolium-5-carboxyanilide.

FRED (OpenEye Scientific Software, Santa Fe, NM), Surflex,[25] and LigandFit[26] (Accelrys Inc., San Diego, CA). The 2005 release of the ChemBridge database (over 400000 compounds) was first filtered using our tool FAF-Drugs[27] and the program FILTER 1.0.2 (Openeye Scientific Software, Santa Fe, NM) in order to remove undesirable compounds (i.e., a very soft filtering protocol was applied). A library containing over 300000 compounds was generated and converted to 3D (up to 50 conformers per compound) using OMEGA (Openeye Scientific Software, Santa Fe, NM). The first docking step was carried out using the rigid-body docking program FRED to generate a library containing molecules having appropriate shape complementarity with the search zone defined around the Thr1 of the proteasome CT-L active site. The top 100000 FRED compounds were then redocked and scored using the program Surflex. Then the 10000 Surflex-top ligands were fully redocked with LigandFit and the molecules were then scored with LigScore1. Two distinct compound lists were created, the Surflex top ranked compounds and the LigandFit (LigScore1) top ranked compounds. After visual inspection of the poses, we selected 200 compounds present in both lists from the top 3000 scored molecules (so-called consensus compounds). Several molecules found to be active in vitro were redocked with the new version of Surflex[16] and further investigated with MolDock.[19] The target structure and docked posed were analyzed interactively using Insight II (Accelrys Inc., San Diego, CA), PyMol (DeLano Scientific, Palo Alto, CA), and Chimera.[28] Molecular volumes were computed with MSM.[29] Some compounds that cross-reacted with T-L and PA sites were also redocked in these binding pockets in a attempt to gain additional insights over possible binding modes of these molecules.

Materials. The compounds selected by virtual ligand screening were purchased from ChemBridge corporation (www.chembridge.com). Purity of compounds **2**−**8** was verified by means of HPLC, using a Waters 600 instrument with a photodiode array detector (chromatograms extracted at 254 and 300 nm), a reversed phase column (X-Terra RP C18, 5 mM, 250 mm × 4.6 mm), and two different eluting systems (MeOH or acetonitrile/water mixture). Results (method, retention time, purity) are summarized in Table 1 of the Supporting Information. All compounds were of purity equal to or greater than 95%, with the exception of compound **3a** (93% purity) and compound **5b** (94% purity). Two hundred stock solutions (10 mM) were prepared by dissolving the corresponding pure solid compounds in DMSO and stored at −20 °C. Rabbit reticulocyte 20S proteasome was obtained from Boston Biochem, Cambridge, MA, and human eythrocyte calpain I from Calbiochem (VWR International SAS, France). The fluorogenic substrates Suc-LLVY-AMC, Boc-LRR-AMC, and Z-LLE-βNA used to measure the proteasome CT-L, T-L, and PA activities, respectively, were purchased from Bachem (France). Other reagents and solvents were purchased from commercial sources. Fluorescence was measured using a BMG Fluostar microplate reader (black 96-well microplates).

Enzyme and Inhibition Assays. Proteasome activities were determined by monitoring the hydrolysis of the appropriate fluorogenic substrate (λ_{exc} = 360, λ_{em} = 460 nm for AMC substrates, and λ_{exc} = 340, λ_{em} = 405 nm for the βNA substrate) for 45 min at 37 °C in the presence of untreated proteasome (control) or proteasome that had been incubated with a test compound. Substrates and compounds were previously dissolved in DMSO, with the final solvent concentration kept constant at 2% (v/v). The buffers were (pH 8): 50 mM Tris, 150 mM NaCl, 10% (v/v) glycerol, 0.01% (w/v) SDS, and 2% (v/v) DMSO (CT-L and PA activities); 50 mM Tris, 150 mM NaCl, 10% (v/v) glycerol, and 2% (v/v) DMSO (T-L activity). The final concentrations were 0.3 nM (20S proteasome), 50 μM (Suc-LLVY-AMC), and 100 μM (Boc-LRR-AMC and Z-LLE-βNA). Using the appropriate substrate, the 200 compounds (0.1−100 μM) were tested in duplicate for each inhibitor concentration to detect their potential to inhibit the CT-L, T-L, and PA activities. The enzyme and the inhibitors were incubated for 15 min before the determination of the enzyme activity. Initial rates determined in control experiments (V_0) were considered to be 100% of the peptidase activity; initial rates (V_i) that were above 100% in the presence of a tested compound were considered to be activations (expressed as activation factor), while initial rates below 100% were considered to be inhibitions. The inhibitory activity of compounds was expressed as IC_{50} (inhibitor concentrations giving 50% inhibition). The values of IC_{50} were calculated by fitting the experimental data to the equation % inhibition = $100(1 - V_i/V_0) = 100\,[I]_0/(IC_{50} + [I]_0)$ or equation % inhibition = $100\,[I]_0^{n_H}/(IC_{50}^{n_H} + [I]_0^{n_H})$; n_H is the Hill number. The activity of calpain I activity in the absence or in the presence of inhibitor was determined using Suc-LLVY-AMC in 50 mM Tris, 2 mM $CaCl_2$, and 10 mM DTT (pH 7.2 and 25 °C).

Characterization of Interaction between Proteasome and Inhibitors. Proteasome (0.3 nM) was incubated with compounds **2**−**4** (30−200 μM) at 37 °C during various time periods (20 s to 45 min, compounds **2** and **3**; 20 s to 200 min, compounds **4**) to block the CT-L activity as shown by the lack of activity against Suc-LLVY-AMC. In a typical experiment, proteasome (0.3 nM) was incubated with compound **2b** (30 μM). Aliquots (90 μL) were withdrawn at intervals from time 0.5 s to time 45 min, and the remaining enzyme activity determined against Suc-LLVY-AMC. When a loss of activity with time occurred, a first-order process characterized by the pseudo-first-order constant k_{obs} was observed. The same experimental conditions were used for control experiments (without inhibitor) but in the presence of the same DMSO percentage as that used for experiments with inhibitor (2% v/v).

Cytotoxicity Assays. HeLa cells (human cervical carcinoma) and HEK-293 cells (human epithelial kidney) were a kind gift from S. Lefebvre (Institut Jacques Monod, Paris) and B. Friguet (UR4-UPMC), respectively. The cells were grown in DMEM supplemented with 10% fetal bovine serum in a 5% CO_2 humidified atmosphere (95% humidity). Confluent cells were collected and then preincubated without inhibitor for 20 h (5×10^3 cells in 100 μL culture medium in 96-well plates). They were then exposed for 48 h to increasing concentrations of compounds: 5−100 μM (final concentration of DMSO: 0.5% v/v). After removal of the DMEM medium, a XTT solution was added to each well (100 μL at 0.3 mg/mL containing 8.3 mM PMS) for 2 h. Absorbance was measured using a BMG Fluostar microplate reader at 485 nm. The cytotoxicity activity of drugs was expressed as the concentration inhibiting cell growth by 50% (EC_{50}) calculated from the survival curves. The experimental data was fitted to the following equation where E is the survival percentage, C the drug concentration, E_{max} is the maximum drug effect, and n is the Hill constant, which describes the shape of the curve: $E = (E_{max} \times C^n)/(C^n + EC_{50}^n)$. EC_{50} is the concentration that produces one-half of the maximum effect.

Acknowledgment. We thank the Institut National de la Recherche Médicale (INSERM) for financial support to L.Q. and Prof. C. Bréchot for creating the Avenir award (B.V.), and the "Association Française contre les Myopathies" (AFM) for a doctoral fellowship (N.B.).

Supporting Information Available: Docked bortezomib molecule and the experimental structure, two-dimensional sketch for molecule **2b**, Inhibition of T-L activity of rabbit proteasome by compounds **3b** and **2c**, PA activity by compounds **7** and **2b** and CT-L activity by compound **7**, HPLC analysis of compounds **2**−**8**. This material is available free of charge via the Internet at http://pubs.acs.org.

References

(1) Coux, O.; Tanaka, K.; Goldberg, A. L. Structure and functions of the 20S and 26S proteasomes. *Annu. Rev. Biochem.* **1996**, *65*, 801–847.

(2) Hershko, A.; Ciechanover, A. The ubiquitin system. *Annu. Rev. Biochem.* **1998**, *67*, 425–479.
(3) Adams, J. The development of proteasome inhibitors as anticancer drugs. *Cancer Cell* **2004**, *5*, 417–421.
(4) Orlowski, R. Z.; Kuhn, D. J. Proteasome inhibitors in cancer therapy: lessons from the first decade. *Clin. Cancer Res.* **2008**, *15;14*, 1649–1657.
(5) Richardson, P. G.; Mitsiades, C.; Hideshima, T.; Anderson, K. C. Proteasome inhibition in the treatment of cancer. *Cell Cycle* **2005**, *4*, 290–296.
(6) Argyriou, A. A.; Iconomou, G.; Kalofonos, H. P. Bortezomib-induced peripheral neuropathy in multiple myeloma: a comprehensive review of the literature. *Blood* **2008**, *112*, 1593–1599.
(7) Borrissenko, L.; Groll, M. 20S proteasome and its inhibitors: crystallographic knowledge for drug development. *Chem. Rev.* **2007**, *107*, 687–717.
(8) Schmidtke, G.; Holzhütter, H.-G.; Bogyo, M.; Kairies, N.; Groll, M.; De Giuli, R.; Emch, S; Groettrup, M. How an inhibitor of the HIV-I protease modulates proteasome activity. *J. Biol. Chem.* **1999**, *274*, 35734–35740.
(9) Furet, P.; Imbach, P.; Fuerst, P.; Lang, M.; Noorani, M.; Koeppler, J.; Zimmermann, J.; Garcia-Echeverria, C. Structure-based optimization of 2-aminobenzylstatine derivatives: potent and selective inhibitors of the chymotrypsin-like activity of the human 20S proteasome. *Bioorg. Med. Chem. Lett.* **2002**, *12*, 1331–1334.
(10) Furet, P.; Imbach, P.; Noorani, M.; Koeppler, J.; Laumen, K.; Lang, M.; Guagnano, V.; Fuerst, P.; Roesel, J.; Zimmermann, J.; Garcia-Echeverria, C. Entry into a new class of potent proteasome inhibitors having high antiproliferative activity by structure-based design. *J. Med. Chem.* **2004**, *47*, 4810–4813.
(11) Basse, N.; Papapostolou, D.; Pagano, M.; Bernard, E.; Felten, A. S.; Vanderesse, R.; Reboud-Ravaux, M. Development of lipopeptides for 20S proteasome inhibition. *Bioorg. Med. Chem. Lett.* **2006**, *16*, 3277–3281.
(12) Groll, M.; Huber, R.; Moroder, L. The persisting challenge of selective and specific proteasome inhibition. *J. Pept. Sci.* **2009**, *15*, 58–66.
(13) Basse, N.; Piguel, S.; Papapostolou, D.; Ferrier-Berthelot, A.; Richy, N.; Pagano, M.; Sarthou, P.; Sobczak-Thepot, J.; Reboud-Ravaux, M.; Vidal, J. Linear TMC-95-based proteasome inhibitors. *J. Med. Chem.* **2007**, *50*, 2842–2850.
(14) Kohno, J.; Koguchi, Y.; Nishio, M.; Nakao, K.; Kuroda, M.; Shimizu, R.; Ohnuki, T.; Komatsubara, S. Structures of TMC-95A-D: Novel proteasome inhibitors from *Apiospora montagnei* Sacc. TC 1093. *J. Org. Chem.* **2000**, *65*, 990–995.
(15) Formicola, L.; Maréchal, X.; Basse, N.; Bouvier-Durand, M.; Bonnet-Delpon, D.; Milcent, T.; Reboud-Ravaux, M.; Ongeri, S. Novel fluorinated pseudopeptides as proteasome inhibitors. *Bioorg. Med. Chem. Lett.* **2009**, *19*, 83–86.
(16) Jain, A. N. Surflex-Dock 2.1: robust performance from ligand energetic modeling, ring flexibility, and knowledge-based search. *J. Comput.-Aided Mol. Des.* **2007**, *21*, 281–306.
(17) Groll, M.; Berkers, C. R.; Ploegh, H. L.; Ovaa, H. Crystal Structure of the Boronic Acid-Based Proteasome Inhibitor Bortezomib in Complex with the Yeast 20S Proteasome. *Structure* **2006**, *14* (3), 451–456.
(18) Palombella, V. J.; Rando, O. J.; Goldberg, A. L.; Maniatis, T. The ubiquitin-proteasome pathway is required for processing the NF-κB1 precursor protein and the activation of NF-κB. *Cell* **1994**, *78*, 773–785.
(19) Thomsen, R.; Christensen, M. H. MolDock: a new technique for high-accuracy molecular docking. *J. Med. Chem.* **2006**, *49*, 3315–21.
(20) Kisselev, A. F.; Callard, A.; Goldberg, A. L. Importance of the different proteolytic sites of the proteasome and the efficacy of inhibitors varies with the protein substrate. *J. Biol. Chem.* **2006**, *281*, 8582–8590.
(21) Berman, H. M.; Westbrook, J.; Feng, Z.; Gilliland, G.; Bhat, T. N.; Weissig, H.; Shindyalov, I. N.; Bourne, P. E. The Protein Data Bank. *Nucleic Acids Res.* **2000**, *28*, 235–242.
(22) Unno, M.; Mizushima, T.; Morimoto, Y.; Tomisugi, Y.; Tanaka, K.; Yasuoka, N.; Tsukihara, T. The structure of the mammalian 20S proteasome at 2.75 A resolution. *Structure* **2002**, *10*, 609–618.
(23) Miteva, M. A.; Lee, W. H.; Montes, M. O.; Villoutreix, B. O. Fast structure-based virtual ligand screening combining FRED, DOCK, and Surflex. *J. Med. Chem.* **2005**, *48*, 6012–6022.
(24) Montes, M.; Miteva, M. A.; Villoutreix, B. O. Structure-based virtual ligand screening with LigandFit: pose prediction and enrichment of compound collections. *Proteins* **2007**, *68*, 712–725.
(25) Jain, A. N. Surflex: fully automatic flexible molecular docking using a molecular similarity-based search engine. *J. Med. Chem.* **2003**, *46*, 499–511.
(26) Venkatachalam, C. M.; Jiang, X.; Oldfield, T.; Waldman, M. LigandFit: a novel method for the shape-directed rapid docking of ligands to protein active sites. *J. Mol. Graphics Modell.* **2003**, *21*, 289–307.
(27) Miteva, M. A.; Violas, S.; Montes, M.; Gomez, D.; Tuffery, P.; Villoutreix, B. O. FAF-Drugs: Free ADME/tox Filtering of compound collections. *Nucleic Acids Res.* **2006**, *34*, W738–744.
(28) Pettersen, E. F.; Goddard, T. D.; Huang, C. C.; Couch, G. S.; Greenblatt, D. M.; Meng, E. C.; Ferrin, T. E. UCSF Chimera—A Visualization System for Exploratory Research and Analysis. *J. Comput. Chem.* **2004**, *25*, 1605–1612.
(29) Sanner, M. F.; Olson, A. J.; Spehner, J. C. Reduced surface: an efficient way to compute molecular surfaces. *Biopolymers* **1996**, *38*, 305–320.